Published in final edited form as:
IEEE MTTS Int Microw Symp. 2004 June ; 3(6-11): 1437–1440.

Analysis and experimental validation of a triaxial antenna for microwave tumor ablation

Christopher L. Brace[1], **Daniel W. van der Weide**[1], **Fred T. Lee Jr.**[2], **Paul F. Laeseke**[2], and **Lisa Sampson**[2]

1 *Department of Electrical and Computer Engineering, University of Wisconsin - Madison*

2 *Department of Radiology, University of Wisconsin - Madison, Madison, WI 53706*

Abstract

We apply a new triaxial antenna for microwave ablation procedures. The antenna consists of a coaxial monopole inserted through an 18-gauge biopsy needle positioned one quarter-wavelength from the antenna base. The biopsy needle creates a triaxial structure, which enhances return loss by more than 10 dB, thus limiting return currents along the feed line. Numerical simulations are used to optimize the antenna design. Numerical and *ex-vivo* experimental results are presented to quantify the field distribution, heating pattern and return loss of the antenna.

Index Terms

Ablation; electromagnetic heating; finite element methods; monopole antennas

I. Introduction

Minimally invasive tissue ablation is becoming an increasingly important tool for the treatment of tumors. The most popular modality, radio-frequency ablation (RFA), has been plagued by high post-treatment local recurrence rates [1]–[6]. In addition, RFA has several drawbacks related to its mode of heating. To create a conduction path, ground pads must be placed on the patient. Risks of superficial burns due to improper pad placement or high input powers, plus additional complexity, make ground pads undesirable. In addition, the impedance of tissue increases with temperature; as a result, tissue charring and long treatment times may be encountered. Tissue charring is a major concern in RFA as it eliminates the conduction path required for heating.

Microwave ablation (MWA), like RFA, uses localized heating to cause tissue necrosis. However, MWA can produce greater, more rapid heating and can easily support the use of multiple probes. The mode of heating in MWA does not rely on a conduction current path, which eliminates ground pad and charring concerns. Lesion size is limited by the available power and treatment time. However, current systems use probes that are too large (14-gauge), and create relatively small zones of necrosis (1.6 cm) [7], which require multiple overlapping ablations.

Most ablation antennas are fed by coaxial lines with small sizes and TEM propagation. Their unbalanced design, however, allows return current flow on the outer conductor. These currents restrict impedance matching and can lead to burns around the insertion point of the probe. If the antenna's input impedance is not matched to the feed line, too much of the applied power is reflected from the antenna and, hence, not deposited in the tissue. The impedance mismatch causes standing waves that can overheat the coaxial feed and cause it to fail.

Other researchers have sought to improve antenna efficiency by using dipoles [8], loaded monopoles [9], and choked monopoles [10]. However, the larger diameter of these antennas makes percutaneous insertion difficult.

The triaxial antenna presented here seeks to not only improve the impedance match between the feed line and antenna, but also to reduce the return currents and subsequent heating along the feed line. In turn, a smaller diameter antenna may be used since the introducing needle is integral to the design.

II. Antenna Design and numerical modeling

A. Antenna geometry

The triaxial antenna design is created from the coaxial antenna and needle together (Fig. 1). The active length of the antenna loaded in tissue (for liver, $\varepsilon_T = 45.6$,σ= 1.97 S/m at 2.45 GHz, 37 °C) is nominally $(2n-1)\ \lambda/4$, where n is an integer. The needle sheath creates the triaxial structure and is positioned $n\lambda/4$ away from the antenna base. Correctly positioning the needle improves return loss and reduces fields flowing back on the coaxial outer conductor. In turn, more energy is deposited in the tissue and less heating of the feed line is encountered.

In order to introduce the antenna percutaneously, a biopsy needle with removable introducer is inserted into the patient. Once the proper needle position has been achieved, the introducer is removed. A coaxial antenna is then inserted through the needle to provide the required tissue heating.

B. Numerical modeling

Finite element modeling (FEM) simulations using commercial software (HFSS) will performed to optimize the antenna design. A model of the triaxial antenna with nominal values of $3\lambda/4$ for the active length and $\lambda/4$ as the insertion depth is created. The antenna is surrounded by a medium with the dielectric properties of either 0.9% saline ($\varepsilon_T = 78$, $\sigma = 1.6$ S/m) or liver tissue and radiation boundary conditions. Simulations will be run using the adaptive mesh technique at a center frequency of 2.45 GHz for $\Delta S < 0.001$. S-parameters are computed for a frequency range of 1–5 GHz using 10000 interpolation points and the iterative method. Once the nominal problem is solved, an optimized model will be computed using Ansoft Optimetrics.

III. Experimental setup

After modeling the triaxial design, antennas are fabricated from low-loss 0.86 mm coaxial cable. First, antennas with an active length of 10.3 mm are inserted into- a 0.9% saline solution and the reflection coefficient (Γ) is measured from S_{11} on an HP8720D vector network analyzer (VNA) from 1–5 GHz. A comparison of a simple coaxial monopole and the triaxial antenna are made. Then, measurements are taken of Γ vs. insertion depth where the needle is either protected from contact with the outer conductor using dielectric tape or left unprotected. In both cases, the insertion depth where Γ is minimized will be recorded and compared to the FEM simulation results.

Next, an antenna with an active length of 12.3 mm is inserted into ex-vivo bovine liver tissue samples. Again, Γ is measured with a VNA and the insertion depth varied until Γ is minimized. At this point, the antenna is connected to a variable power microwave source (Cober-Muegge, LLC). Average powers of 10–40 W are used to ablate the liver tissue for 30 s to 12 min. while the forward and reflected powers are monitored. At the end of the ablation, tissue temperature is measured from a thermocouple probe inserted into middle of the lesion.

NIH-PA Author Manuscript

NIH-PA Author Manuscript

IV. Results

FEM simulations revealed that Γ is minimized for a probe length of 12.3 mm and insertion depth of 3.5 mm in liver tissue. Approximately 14700 tetrahedral elements were required for convergence. The electric field magnitude, normalized to the incident field, is shown in Fig. 2 and illustrates the lack of field at the feed plane.

In 0.9% saline, the optimum length of both the coaxial and triaxial antennas was found to be 10.3 mm. For a 10.3 mm coaxial monopole in saline, Γ was measured to be −35.0 dB at 2.45 GHz. For the same antenna inserted 3.5 mm through an 18-gauge needle, Γ was reduced to −46.2 dB. Thus, the triaxial design improved reflection coefficient by 11.2 dB over the simple coaxial monopole, as shown in Fig. 3.

From Fig. 4, it is clear that the minimum reflection coefficient occurs at the design frequency (2.45 GHz) in both the numerical and empirical cases, though the absolute values of Γ differ slightly. This discrepancy is likely due to a coarse mesh and not enough interpolation points in the simulation model. However, the optimization goal of the simulations was successful.

Experimental validation of the insertion depth optimization is shown in Fig. 5, where Γ is minimized between 3mm and 4mm. Interpolation of each plot reveals that Γ is lowest at an insertion of 3.3 mm for the protected case and at 3.5 mm for the unprotected case.

The antenna was then inserted into ex-vivo bovine liver. After careful trimming of the center conductor length, Γ was measured to be −25.0 dB (0.32% reflected power) for an active length of 12.3 mm. Reflection coefficient is most likely limited by inhomogeneity in the dielectric constant.

Before ablations began, tissue temperatures were measured to be 18.0±0.5 °C. Shortly after ablation, temperatures in the zone of necrosis were measured to be in excess of 80 °C, far surpassing the commonly used metric of ~50 °C for irreversible cell damage.

Fig. 6 shows the results of an 8 minute ablation with the 18-gauge triaxial antenna powered at 25 W. The zone of necrosis measures 2.8+0.1 cm in the transverse direction and 5.5±0.1 cm in the longitudinal direction with a 1.0±0.1 cm "tail." Fig. 7 shows a lesion created with 25 W for 12 minutes with the antenna in place. The lesion measured 3.510.1 cm in the transverse direction and 6.3±0.1 cm in the longitudinal direction.

Reflection coefficients during the procedure were at most −14 dB (i.e., < 4% reflected power) and usually remained near −20 dB (~1%). The increase in Γ was primarily due to the temperature dependence of the tissue dielectric properties.

The lack of necrosis around the feed line indicates that the feed was never heated above ~50 °C. Indeed, measurements on the feed line and connectors in air using a simple thermocouple were no greater than 30 °C during the procedures of Fig. 6 and Fig. 7.

VII. Conclusion

A triaxial antenna design for clinical microwave ablation was presented. Numerical and experimental data provided show that the triaxial antenna achieves return losses as low as −46.2 dB in saline and −25.0 dB in ex-vivo bovine liver tissue, with the triaxial design improving return losses by 11.2 dB over a coaxial design. The antenna is capable of being presented inside an 18-gauge needle, making percutaneous introduction tractable. Because of the improved impedance match heating along the feed line was negligible. Elliptical-shaped lesion sizes of 5.5x2.8 cm and 6.3x3.5 cm were achieved with 25 W for 8 and 12 minutes, respectively.

Standard RF ablation times are ~12 minutes and lesions using a single, water-cooled probe are typically about 3.5x2.5–3 cm. Thus, we find that MWA with this antenna is capable of faster, more effective ablation of liver tumors.

Acknowledgements

This research is supported by the NIH. The authors wish to thank Dieter Haemmerich for discussions related to this work.

References

1. Lencioni R, Cioni D, Bartolozzi C. Percutaneous radiofrequency thermal ablation of liver malignancies: techniques, indications, imaging findings, and clinical results. Abdom Imaging 2001;26:345–60. [PubMed: 11441546]
2. Izzo F, Barnett CC Jr, Curley SA. Radiofrequency ablation of primary and metastatic malignant liver tumors. Adv Surg 2001;35:225–50. [PubMed: 11579813]
3. Horigome H, Nomura T, Nakao H, Fujino 'N, Murasaki G, Kanematsu T, Joh T, Ohara H, Itoh M. Percutaneous radio-frequency ablation therapy using a clustered electrode for malignant liver tumors. J Clin Gastroenterology 2001;32:418–22.
4. Gillams AR. Thermal ablation of liver metastases. Abdom Imaging 2001;26:361–8. [PubMed: 11441547]
5. de Baere T. Radio-frequency ablation of the liver. AJR Am J Roentgenol 2001;177:1213–5. [PubMed: 11641207]
6. Solbiati L, Livraghi T, Goldberg SN, lerace T, Meloni F, Dellanoce M, Cova L, Halpern EF, Gazelle GS. Percutaneous radio-frequency ablation of hepatic metastases from colorectal cancer: long-term results in 117 patients. Radiology Oct;2001 21(1):159–66. [PubMed: 11568334]
7. Seki T, Wakabayashi M, Nakagawa T, et al. Ultrasonically guided percutaneous microwave coagulation therapy for small hepatocellular carcinoma". Cancer 1994;74:817–25. [PubMed: 8039109]
8. Casey JP, Bansal R. The near-field of an insulated dipole in a dissipative dielectric medium. IEEE MTT April;1986 34(4):459–63.
9. Labonte S, AH H, Roy L. Monopoles for microwave catheter ablation of heart tissue. IEEE MTT Symp Dig 1995:303–306.
10. Lin JC, Wang Yu-Jin. 'The cap-choke catheter antenna for microwave ablation treatment. IEEE Trans Biomed Eng June;1996 43:657–60. [PubMed: 8987271]

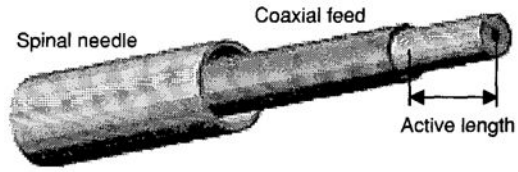

Fig. 1.
Coaxial antenna inserted through a biopsy needle.

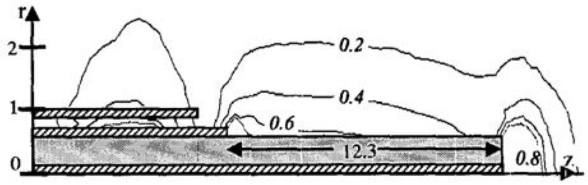

Fig. 2.
Normalized electric field magnitudes of a triaxial antenna. Axis dimensions in (mm).

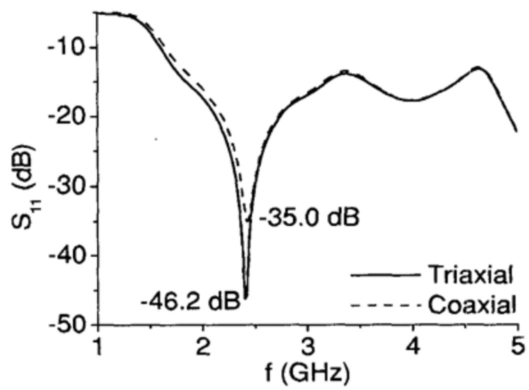

Fig. 3.

Measured S_{11} of a coaxial monopole and a triaxial antenna. The triaxial design reduces reflections by 11.2 dB.

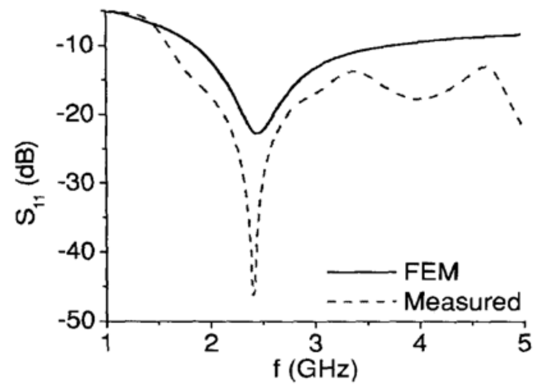

Fig. 4.
Comparison of an FEM simulation and VNA measured measurement of the triaxial antenna.

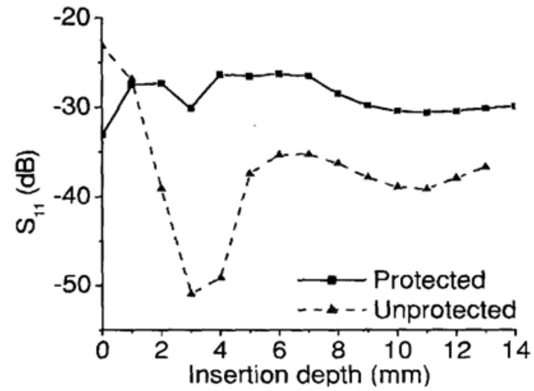

Fig. 5.

Insertion depth vs. Γ measurements. Γ is minimized at 3.5 mm insertion depth.

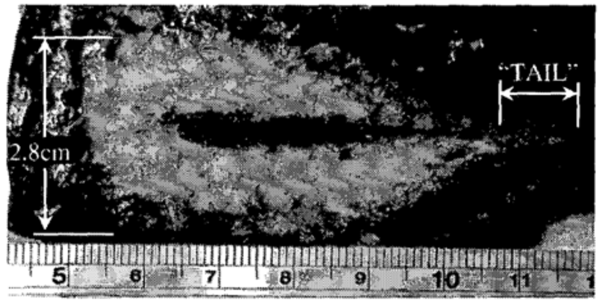

Fig. 6.

Necrosis due to a 25 W, 8 minute ablation using the triaxial antenna.

NIH-PA Author Manuscript

NIH-PA Author Manuscript

Fig. 7.
Necrosis due to a 25 W, 12 minute ablation using the triaxial antenna.